J. Biochem. 2013;153(5):431–439 doi:10.1093/jb/mvt016

JB THE JOURNAL OF BIOCHEMISTRY

Trypanosoma brucei 14-3-3I and II proteins predominantly form a heterodimer structure that acts as a potent cell cycle regulator *in vivo*

Received December 28, 2012; accepted January 22, 2013; published online March 1, 2013

Masahiro Inoue[1,*], Kouichi Yasuda[1], Haruki Uemura[2], Natsumi Yasaka[1], Achim Schnaufer[3], Mihiro Yano[4], Hiroshi Kido[4], Daisuke Kohda[5], Hirofumi Doi[6], Toshihide Fukuma[1], Akihiko Tsuji[7] and Nobuo Horikoshi[8]

[1]Department of Infectious Medicine, Division of Eukaryotic Microbiology, Kurume University School of medicine, 67 Asahi-machi, Kurume, Fukuoka 830-0011, Japan; [2]Institute of Tropical Medicine, Nagasaki University, 1-12-4 Sakamoto, Nagasaki 852-8523, Japan; [3]Institute of Immunology & Infection Research, University of Edinburgh, King's Buildings, Ashworth Laboratories, West Mains Road, Edinburgh EH9 3JT, UK; [4]Division of Enzyme Chemistry, Institute for Enzyme Research, University of Tokushima, 3-18-15 Kuramoto-cho, Tokushima, 770-8503 Japan; [5]Division of Structural Biology, Medical Institute of Bioregulation, Kyushu University, 3-1-1 Maidashi, Fukuoka, Japan; [6]Celestar Lexico-Sciences, Inc, 5-9-9 Toukoudai, Tsukuba, Ibaraki 300-2635, Japan; [7]Department of Biological Science and Technology, University of Tokushima Graduate School, 2-1 Minamijosanjima, Tokushima 770-8506, Japan; and [8]Division of Molecular Radiation Biology, Department of Radiation Oncology, University of Texas Southwestern Medical School, 5323 Harry Hines Blvd., Dallas, TX 75390, USA

*Masahiro Inoue, Department of Infectious Medicine, Division of Eukaryotic Microbiology, Kurume University School of Medicine, Asahi-machi, Kurume, Fukuoka 830-0011, Japan.
Tel: +81-942-31-7550, Fax: +81-942-31-0344,
email: inouedna@med.kurume.u-ac.jp

Hetero- and homodimerization of 14-3-3 proteins demonstrate distinctive functions in mammals and plants. *Trypanosoma brucei* 14-3-3I and II (Tb14-3-3I and II) play pivotal roles in motility, cytokinesis and the cell cycle; however, the significance and the mechanism of Tb14-3-3 dimerization are remained to be elucidated. We found that ectopically expressed epitope-tagged Tb14-3-3I and II proteins formed hetero- and homodimers with endogenous Tb14-3-3I and II proteins. However, we also found the ability to form hetero- or homodimers between Tb14-3-3I and II proteins was clearly affected by the sequence and location of the epitope tag used. We found a blue native polyacrylamide gel electrophoresis system followed by western blotting may distinguish monomer from dimer structure, and stable from unstable conformation of Tb14-3-3. Combined with co-immunoprecipitation results, we revealed that Tb14-3-3 proteins mainly existed as heterodimeric form. Furthermore, co-overexpression of Tb14-3-3I and II proteins in *T. brucei* induced aberrant numbers of organelles in cells, but overexpression of either isoform alone rarely produced such morphology. These results suggest that heterodimers play more significant roles than homodimers not only in the maintenance of steady-state levels of the 14-3-3 proteins but also in the regulation of cytokinesis.

Keywords: 14-3-3/cell division/cytokinesis/dimerization/*Trypanosoma brucei*.

Abbreviations: Ab, antibody; BN-PAGE, blue native polyacrylamide gel electrophoresis; BSFs, bloodstream forms; CBB, Coomassie brilliant blue; PCFs, procyclic forms; Tb, *Trypanosoma brucei*.

Trypanosoma brucei is a protozoan kinetoplasid organism that is the casual agent of sleeping sickness in humans and Nagana disease in cattle. The disease is spread by the bite of the tsetse fly, in which procyclic forms (PCFs) of the parasite proliferate and differentiate into bloodstream forms (BSFs), the life cycle stage that proliferates in the mammalian host. The disease is fatal if left untreated, and no effective drug is currently available to treat the late stage of the disease (*i.e.* involvement of the central nervous system).

14-3-3 proteins are a group of dimeric acidic proteins with a relative molecular mass of 30 kDa. These proteins are expressed in all eukaryotic organisms and act as molecular chaperones to modify many biological processes, including the cell cycle, signal transduction, intracellular trafficking/targeting, transcription, host defense and cell death. Over 200 proteins interacting with 14-3-3 proteins have been discovered (*1*), and most of the interactions are mediated through well-conserved or related phosphorylated Ser/Thr peptide motifs (*2–4*). We have previously shown that *T. brucei* 14-3-3 proteins play essential roles in motility, cytokinesis and the cell cycle (*5*). Most organisms contain more than 1 isoform; there are 2 isoforms in yeast and trypanosome (*5*), 7 isoforms in mammals and at least 15 isoforms of 14-3-3 in plants (*6*). Combinations of 14-3-3 dimers may potentially give rise to some molecular diversity of 14-3-3, although there are a limited number of possible hetero- and homodimer combinations (*7*). To date, most of the work involving the distinctive patterns of human and budding yeast 14-3-3 intraspecies dimers has used artificially peptide-tagged 14-3-3 proteins (*8*), which may have altered the tendency of the 14-3-3 proteins to dimerize in homo and hetero forms *in vivo*, as shown in this study. Thus, proportions of hetero- and homodimerized 14-3-3 proteins are still unknown in most organisms. Our method used in this study—blue native polyacrylamide gel electrophoresis (BN-PAGE) of 14-3-3 proteins followed by western blotting with isoform-specific antibodies—may circumvent the

problems of the peptide-tagging approach in the case of *T. brucei* 14-3-3 proteins. Although 14-3-3 exists mainly in dimeric forms in most organisms, recent interesting reports have shown that serine phosphorylation (Ser 58 in the human ζ isoform) of mammalian 14-3-3 by several kinases, including MAPKAP kinase 2 (*9*), protein kinase B/Akt (*10*) and sphingosine-dependent kinase (*11*), disrupts 14-3-3 dimerization in cells (*12*); however, some controversy still exists (*13*). The role of monomeric mammalian 14-3-3 proteins remains unclear. Notably, *T. brucei* 14-3-3I and II lack the corresponding serine residue (Ser 58 in the human ζ isoform) and the other conserved amino acid residues required for dimerization (*14*).

We show here that most of the *T. brucei* 14-3-3 forms heterodimers *in vivo* and the heterodimerized form may play a more important role than the monomeric and homodimeric forms in terms of cytokinesis.

Materials and Methods

Co-expression and purification of 14-3-3I and GST-14-3-3II

The coding sequences of 14-3-3I and II were obtained by PCR and inserted into pRSFDuet-1 at the NdeI and EcoRV sites for the expression of non-tagged 14-3-3I protein, and pGEX7P-1 at the ApaI and Sma I sites, which carried a point mutation eliminating the ApaI site in the *LacIq* gene of pGEX6P-1 (GE Healthcare). BL21 (DE3)-derived T7 express lysY/I^q competent cells (New England Biolabs, Japan) were simultaneously transformed with pRSFDuet-1 and pGEX7P1 constructs. Glutathione S-transferase (GST)-fusion protein induction was carried using 0.4 mM isopropylthio-β-galactoside (IPTG) at 30°C for 3 h. The affinity purification of GST-fusion proteins was carried out using glutathione beads (GE Healthcare) and 0.1 mM DTT containing PreScission protease digestion buffer (GE Healthcare). The glutathione beads were then extensively washed with PreScission protease digestion buffer containing 0.5 M NaCl. Finally, purified proteins were eluted with 20 mM reduced glutathione (Sigma). To obtain the heterodimerized 14-3-3 proteins without GST-tag, PreScission protease digestion was carried out according to the protocol supplied by GE Healthcare. After the digestion, two extra amino acid residues (Gly–Pro) remained in the N-terminus of the 14-3-3 proteins.

Expression and purification of human 14-3-3ζ and mutants

Human 14-3-3ζ and mutants were expressed in BL21 (DE3) *Escherichia coli* as His-tag fusion proteins using pET-47b. After affinity purification with cobalt beads, His-3 C protease was used to remove the His-Tag. After digestion, undigested proteins and 3C protease were removed using cobalt beads. The purified samples without the peptide tag (only two extra amino acid residues remained in the N-terminus) were dialysed against the following buffer: 100 mM NaCl and 50 mM HEPES–HCl pH 7.5.

BN-PAGE analyses of the dimerization status of T. brucei 14-3-3 proteins

BN-PAGE analyses were carried out according to the manufacturer's manual (Invitrogen). Cells (5×10^7) were lysed with 100 µl of 1% digitonin-containing PEME buffer (0.1 M PIPES pH 6.9, 2 mM EGTA, 1 mM $MgSO_4$, 0.1 mM EDTA and 0.1 mM DTT) on ice for 30 min. After centrifugation at 5,000 rpm for 5 min at 4°C, the supernatants were transferred to new tubes and spun again at 15,000 rpm for 5 min at 4°C. One microlitre of each supernatant was transferred to a new tube and mixed with 5 µl of NativePAGE Sample Buffer (Invitrogen) (×4), 14 µl of 1% digitonin-containing PEME with 0.1 mM DTT and 1 µl of 5% G-250 sample additive. For the analyses of recombinant proteins, 1 µl of recombinant protein was added instead of cell lysates, as noted earlier. Samples were separated on native PAGE Novex gels (4–16%) (Invitrogen) at 150 V for 170 min. NativeMark Unstained Protein Standard (Invitrogen) was used to estimate the relative molecular weights of the protein complexes. Gels were transferred to polyvinylidene difluoride (PVDF) membranes in 0.1% SDS-containing transfer buffer. The membranes were stained with Ponceau S, destained extensively with dH_2O, incubated with Immunoblock (DS Pharma Biomedical) and then incubated with antiserum and antibodies against I, II and τ isoforms of 14-3-3.

Establishment of pLew82 T7phleo I- and/or pLew82 T7puro II-transfected 29-13 PCF cells

The coding sequences of 14-3-3I and II were subcloned into pLew82 T7phleo (phleomycin-resistant) and pLew82 T7puro (puromycin-resistant) vectors. The constructs were transfected into 29-13 cells and selected with phleomycin and/or puromycin (*15*). Three clones were established for each construct, and examined for cell growth and morphological changes. The data presented are representative of all three clones.

The construction and modification of the expression vectors, along with the regular methods for fusion protein expression and purification used in this study, are described below.

6xMyc 14-3-3 expression vectors

14-3-3 cDNAs designated as I, II, and human 14-3-3τ were amplified using LA Taq (TAKARA Bio) with the following primers: I, sense, 5′-CGAATTCATGACGGACTGCATCAAGT-3′, antisense, 5′-GGTCTCCACCCTTGTCAGTT-3′; II, sense, 5′-CGGAATTCATGGCGGGCTTTCAAATAC-3′, antisense, 5′-GAGCTCACTCCAATTCCTCCATC-3′; τ, sense, 5′-GAATTCATGGAGAAGACTGAGCTGATCC-3′, antisense, 5′-CTTAGTTTTCAGCCCCTTCTGCCGCAT-3′.

PCR products were subcloned into pGEM-T Easy vector, and sequences were checked as described earlier. Each EcoRI-digested cDNA fragment was subcloned into pcDNA3-6xmyc vectors (gift from Dr Kunihiro Tsuchida). Inserts containing 6xmyc were subcloned into the pKI-7 vector as described below.

Construction of pLew82 EYFP-difopein

pEYFP-difopein (pscm138) (received from Dr Haian Fu) was digested with NotI, blunted and self-ligated. The resultant vector was digested with NheI, blunted and digested with BamHI. The EYFP-difopein fragment was purified and ligated with pLew 82 at HindIII (converted to a blunt end) and BamHI sites.

Construction of C-terminally 2xMyc tagged 14-3-3 expressing plasmid

Coding sequences of 14-3-3I or II without stop codon were subcloned in pcDNA3 2xmyc vector. The coding sequences with 2xmyc were amplified and inserted into pLew82. All the sequences were verified.

Construction of T. brucei T7 polymerase-based expression vector pKI-7 (non-inducible expression vector with medium expression levels)

Aldolase splicing acceptor sequence (SAS) was isolated from pT11-bs with SmaI and HindIII digestion and inserted into pSP73 (Promega), which is designated as pKI-0. The 2XTetO cassette was designed to anneal to the following oligonucleotides: 5′-TCGAGTCCCTATCAGTGATAGAGATCTCCCTATCAGTGATAGAGC-3′ and 5′-GCTCTATCACTGATAGGGAGATCTCTATCACTGATAGGGAC-3′. Annealed oligonucleotide was then inserted into pKI-0 at the XhoI and SmaI sites. The T7 terminator oligonucleotides 5′-GATCCCTAGCATAACCCCTTGGGGCCTCTAAACGGGTCTTGAGGGGTTTTTTGTAT-3′ and 5′-ATACAAAAAACCCCTCAAGACCCGTTTAGAGGCCCCAAGGGGTTATGCTAGG-3′ were annealed and inserted into the BamHI and EcoRV sites. The resultant plasmid was amplified by PCR using a T7 promoter oligonucleotide and the primer 5′-ATACAAAAAACCCCTCAAGAC-3′. The PCR product was inserted into pBluescript II KS (+) at a blunted BssHII site, and this vector was designated pKI-2. pKI-2 was amplified by PCR using M13 forward and reverse primers and digested with BamHI. The resultant fragment containing the T7 promoter and 2xTetO was inserted into pLew100 at blunted KpnI and BamHI sites. The 3′-untranslated region plus 2xT7 terminator was isolated from pLew111 by StuI digestion followed by blunting and NheI digestion. This fragment was then inserted into pLew100 containing the T7 promoter, 2xTetO and aldolase SAS at blunted BamHI and NheI sites. The plasmid

construct was designated pKI-6. pKI-7 was made by swapping the XhoI–HindIII fragment of pKI-0 with the XhoI–HindIII fragment of pKI-6, and used for this study. Tet did not regulate T7 promoter activity in spite of the presence of the 2xTetO sequence; therefore, we used this vector as a non-inducible expression vector. The expression levels of this vector were ~1/7 of those of pLew82 in the presence of 1 μg/ml Tet (data not shown).

Modification of pLew82 vector (pLew82 T7) and construction of pLew 82T7-I and II

The pLew82 vector was modified by the insertion of annealed oligonucleotides of weak T7 promoter at the BamHI site. The sequences of oligonucleotides are as follows: 5′-GATCCTTAATACGTCTCA CTATAGGGA-3′ and 5′-GATCTCCCTATAGTGAGACGTATT AAG-3′. Permanent transfectants with pLew82 T7 vector do not require 1 ng/ml Tet for maintenance of the clones, whereas pLew82 transfectants do. cDNA inserts were amplified with the following primers using Phusion polymerase (Finnzyme): I, 5′-GAATA AGCTTAAACAATGACGGACTGCATCAAGTGGTAC-3′ and 5′-GTCAGTTCACGGGTTGCTCGTCAGTCCAGA-3′; and II, 5′-CTCAAGCTTGCGGTTAAAATGGCGGGCTTTCAAATAC CTG-3′ and 5′-CCTCACTCCAATTCCTCCATCGCAGTTC-3′. The amplified products were digested with HindIII and inserted into pLew82T7 at BamHI (converted to a blunt end) and HindIII sites of pLew82T7puro and pLew82T7phleo, respectively. All sequences were verified.

Recombinant protein expression and western blotting analyses

Recombinant proteins were expressed in DH5α and/or BL21 cells, and purified according to the manufacturers' protocols. The proteins were separated by 10–20%, or 4–20% gradient SDS–PAGE (Daiichi, Japan), and either stained with Coomassie brilliant blue (CBB) or electrophoretically transferred to PVDF membranes (Millipore). Membranes were blocked with either 4% non-fat milk or Block-Ace (DS Pharma Biomedical, Japan). Anti-sera against *T. brucei* 14-3-3I and II were obtained from Wistar rats by immunization with 250 μg of purified GST-I and GST-II fusion proteins with Complete Freund Adjuvant, respectively (*5*). Anti-I serum was precleared with GST-human 14-3-3 and GST-II proteins. Anti-II serum was precleared with GST-human 14-3-3 and GST-I proteins. The secondary antibodies peroxidase AffiniPure F(ab′)2 Fragment Goat anti-Rat Fc (gamma), peroxidase-conjugated AffiniPure F(ab′)2 Fragment Goat Anti-Mouse IgG (H + L) and peroxidase-conjugated AffiniPure F(ab′)2 Fragment Donkey Anti-Rabbit IgG (H + L) were all purchased from Jackson ImmunoResearch. Primary antibodies, including α-Myc 9E11 (NeoMarkers), α-human 14-3-3: K19 (Santa Cruz) and α-14-3-3τ: C-17 (Santa Cruz), were purchased and used according to the manufacturers' protocols. Anti-I and II rat sera were diluted 1–2,000-fold with TTBS (50 mM Tris pH 7.5, 150 mM NaCl and 0.02% Tween 20) containing 20% Block Ace or Immunoblock (DS Pharma Biomedical). Secondary antibodies were diluted 20,000-fold with TTBS. Blots were visualized with X-ray films using Super Signal West Pico chemiluminescent substrate (PIERCE). For transfection, HEK293T cells were grown in Dulbecco's modified Eagle's medium supplemented with 10% FCS and 20 μg/ml of gentamicin (GIBCO BRL). Sixteen hours before standard transfection with FuGENE 6 Transfection Reagent (Roche), 5×10^5 of human HEK293T cells per well were seeded onto six-well culture dishes. Two days after transfection, the cells were lysed with the BN-PAGE buffer as described earlier.

Establishment and analyses of N-terminal 6xMyc-I-, II- or τ-expressing, and C-terminal I-2xMyc- or II-2xMyc-expressing 29-13 PCF cell clones

pKI-7 was digested with BamHI and blunted with T4 DNA polymerase before being subjected to HindIII digestion. The HindIII- and EcoRV-digested fragments isolated from pcDNA3 6xmyc-I, -II and 14-3-3τ were then inserted into the resultant predigested pKI-7. The final constructs were designated as pKI-7 6xmyc-I, -II and -τ.

Transfection of pKI-7 6xmyc-I, -II, -τ, pLew82 I-2xmyc, pLew82 II-2xmyc, pLew82T7puro I or pLew82T7phleo II into 29-13 PCF cells expressing TetR and T7 polymerase, was carried out using an electroporation method as described earlier (*15*). Phleomycine selection was started 1 day after transfection in multiwell 96-well (Becton Dickinson, Falcon) plates. About 5–10 clones were isolated from each plate within 2 weeks. The expression of proteins was checked by western blotting using α-14-3-3I serum, α-14-3-3II serum and α-Myc antibody. Clones with high expression levels were used for further studies. Immunoprecipitation and western blotting were carried out as follows: 1×10^8 cells were washed three times with ice cold PBS (−) (Sigma) and lysed using 100 ml of NP-40 lysis buffer: 0.5% NP-40, 150 mM NaCl, 10 mM Tris–HCl pH 7.5, 5 mM EDTA, 50 mM NaF, 1 mM $NaVO_4$ and a protease inhibitor cocktail (Roche). Lysates were cleared twice by low-speed and high-speed centrifugations. Ten microlitre was kept for western blot analysis (input), and 400 μl of NP-40 lysis buffer was added to each sample. Each sample was then subjected to immunoprecipitation using 1 μg of α-Myc antibody followed by 5 μl of rec-Protein G beads (ZYMED). Precipitated samples were washed three times, transferred to a vacant Auto-Seq G50 column (GE Healthcare) and spun at 5,000 rpm to drain the NP-40 lysis buffer. After drainage of the lysis buffer, 20 μl of 1 × SDS sample buffer containing 2-mercaptoethanol was added, the column was left to sit for 5 min and then spun at 5,000 rpm for 1 min. The samples were then boiled and separated by SDS–PAGE followed by western blotting as described earlier. Western blot analysis was carried out using Myc-peptides elutes and antisera against 14-3-3I and II.

Results

Evaluation of BN-PAGE for the analyses of 14-3-3 dimerization

The analyses of *T. brucei* cells expressing Myc-tagged versions of 14-3-3 isoforms indicated that the proteins form hetero- and homodimers in *T. brucei* (Supplementary Figs S1 and S2), which is dependent of the sites and the length of the tags. Other peptide-tagging approach of *T. brucei*14-3-3 produced different dimerization preferences, which are also dependent of the sites and the sequences of the peptide-tags (data not shown).

The BN-PAGE system uses Coomassie G-250 as the charge molecule, which binds to the proteins and confers a net negative charge during PAGE, while maintaining the proteins in their non-denatured native state. Thus, BN-PAGE can discriminate the molecular masses of native proteins more precisely than native PAGE (*16*). The BN-PAGE system combination with western blotting was evaluated whether it can discriminate the conformations of these isoforms of *T. brucei* 14-3-3 proteins under physiological conditions, that is, without artificial peptide tags or overexpression.

First, we evaluated whether this system could be applied for the detection of dimerization of 14-3-3 proteins using purified recombinant untagged human ζ isoform and the following mutants: ζ K49E, which is known to show intact dimerization but defective phosphoserine binding (*17*), and ζ S58D, which is known to show hampered dimerization (*18*). A single discrete band of 55 kDa that bound G-250 CBB was detected in the lanes of 14-3-3ζ and 14-3-3ζ K49E but not 14-3-3ζ S58D, regardless of the protein concentration (Fig. 1A). This indicated that BN-PAGE is capable of detecting stable dimeric forms of recombinant 14-3-3 proteins as a single discrete band, and that it is suitable for the analysis of 14-3-3 conformations under native conditions. We found that monomeric or loosely structured 14-3-3 proteins, for example, the ζ S58D mutant, seem to have higher affinity for G-250 than tightly structured homodimeric forms, which may give rise to a smear representing an unusual complex of the detergent-bound form of G-250 with monomeric or

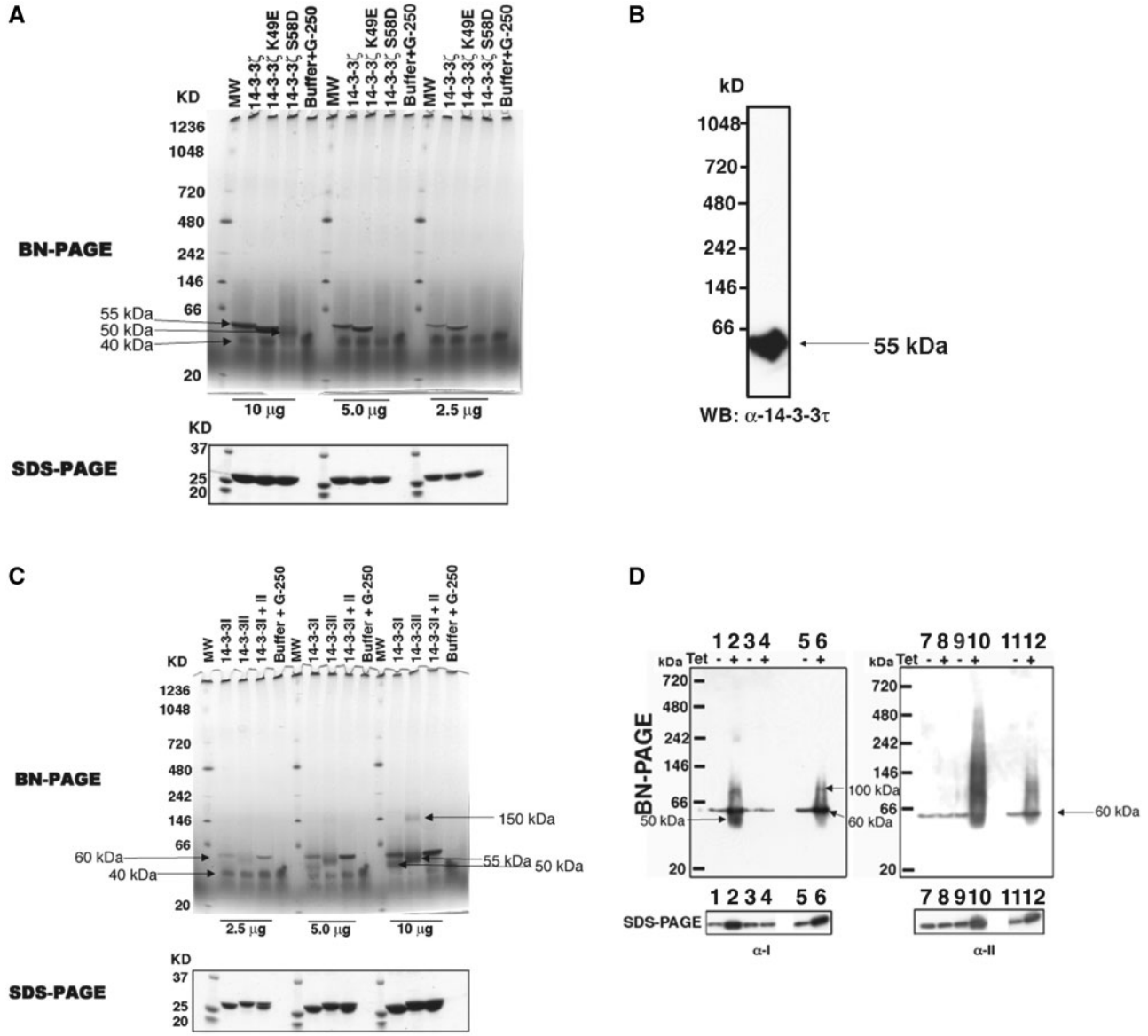

Fig. 1 (**A**) BN-PAGE analyses of purified human 14-3-3ζ and mutants. Each sample was separated by BN-PAGE, and gels were destained. The same samples were separated by SDS–PAGE followed by staining with CBB. The amounts and names of the mutants are indicated. (**B**) BN-PAGE analyses of Jurkat T cells. Cell lysates were subjected to BN-PAGE followed by western blotting using the indicated antibodies. A band of ~55 kDa, corresponding to the size of dimeric human14-3-3τ, is detected. (**C**) BN-PAGE analyses of purified I, II and I + II heterodimeric proteins. The purified recombinant proteins without the peptide tag (only two extra amino acid residues remained in the N-terminus) were dialysed against the following buffer: 100 mM NaCl and 50 mM HEPES–HCl pH 7.5. Each sample was separated by BN-PAGE, and gels were destained. The same samples were separated by SDS–PAGE followed by staining with CBB. The amounts and names of proteins are indicated. (**D**) BN-PAGE analyses of Tet-inducible 14-3-3I, 14-3-3II or 14-3-3I + II expressing clones. The same amounts of cell lysates ($\sim 5 \times 10^5$ cells/lane) on Day 1 following Tet-uninduction Tet (−) or induction Tet (+) were subjected to BN-PAGE followed by western blotting using the indicated isoform-specific antisera (α-14-3-3I: lanes 1–6, α-14-3-3II: lanes 7–12). The amounts of membrane-transferred proteins were confirmed by Ponceau S staining (data not shown). Each lane represents as follows; lanes 1 and 7, Tet-inducible 14-3-3I overexpressing clone F2 Tet (−); lanes 2 and 8, Tet-inducible 14-3-3I overexpressing clone F2 Tet (+); lanes 3 and 9, Tet-inducible 14-3-3II overexpressing clone B8 Tet (−); lanes 4 and 10, Tet-inducible 14-3-3II overexpressing clone B8 Tet (+); lanes 5 and 11, Tet-inducible 14-3-3I + II overexpressing clone A11 Tet (−); lanes 6 and 12, Tet-inducible 14-3-3I + II overexpressing clone A11 Tet (+).

loosely structured 14-3-3ζ S58D proteins (Fig. 1A). Of note, the increases in the intensities of smears are concomitant with decreases in the intensity of a band at 40 kDa, corresponding to the detergent-bound form of G-250 (Fig. 1A, the lanes labelled as 14-3-3ζ S58D and Buffer + G250). Therefore, we then applied this method to detect dimerization in extracts from living cells by investigating the human 14-3-3τ isoform in Jurkat T cells. 14-3-3τ protein is known to be abundantly expressed and may exist mainly as a homodimeric form in Jurkat cells (*19*). A single 55 kDa band was detected using an antibody against the τ isoform (Fig. 1B), indicating that BN-PAGE is suitable for the analysis of 14-3-3 conformation in cell lysates. Dimerized 14-3-3 in the Jurkat T cells appeared as a discrete band without a detectable protein smear, suggesting that higher-order complexes of 14-3-3 protein(s), namely, complexes of dimerized 14-3-3τ

proteins and their binding proteins, are not detected in this system, possibly because most of 14-3-3τ proteins exist as dimers.

Then, to identify the structures of *T. brucei* 14-3-3 proteins *in vitro*, we used an *E. coli* co-expression and purification system. All the purified recombinant proteins used in the BN-PAGE analyses were untagged. Purified 14-3-3I showed the band of 60 kDa with a detectable protein smear. The intensity of the band of 60 kDa of the homodimerized 14-3-3I is less than that of the heterodimerized band of 14-3-3I + II (Fig. 1C, lanes of 14-3-3I and 14-3-3I + II). Within this smear, more intense bands corresponding to 50 kDa were detected when 5.0 μg of purified 14-3-3I was applied and more apparently when 10 μg was applied (Fig. 1C). The 50-kDa band which migrate faster than the 14-3-3I homodimer (60 kDa band) and slower than the detergent-bound form of G-250 (40 kDa band), could be complexes of singular 14-3-3I and detergent-bound CBB G-250 (Fig. 1C, compare lanes labelled Buffer + G-250 and 14-3-3I). These results also indicate that the homodimer of 14-3-3I is not as stable as the heterodimers of 14-3-3I and 14-3-3II (14-3-3I + II). That is why, in the presence of 14-3-3II, 14-3-3I may make the heterodimer more efficiently than the homodimer. Purified 14-3-3II appeared as a smear, similar to the 14-3-3ζ S58D mutant (Fig. 1A), when 2.5 μg of purified 14-3-3II was applied, suggesting that homodimerization of 14-3-3II scarcely occurs at low protein concentrations. 14-3-3II forms homodimers less readily than 14-3-3I, as shown by the fact that a band of dimeric 14-3-3I is visible at this protein level (2.5 μg), while the smear is more prominent for 14-3-3II (Fig. 1C). When 5.0 or 10 μg of purified 14-3-3II was applied, a diffuse band of 55 kDa with a protein smear of 50–150 kDa and a diffuse band of 150 kDa appeared concomitant with a decrease in the intensity of the band of 40 kDa corresponding to the detergent-bound G-250 (Fig. 1C, compare the lanes labelled Buffer + G-250 and 14-3-3II). The data suggest that monomer and a loosely structured dimer of 14-3-3II can tightly complex with the detergent-bound form of G-250, which might give rise to the band of ~55 and ~150 kDa, respectively, when high concentrations of the protein were applied (5.0 or 10 μg of purified 14-3-3II). On the contrary, the co-expressed and co-purified 14-3-3I + II complexes run as a single discrete 60 kDa band regardless of the concentrations of the proteins (Fig. 1C), suggesting that the most stable structure of *T. brucei* 14-3-3 is the heterodimer when both isoforms are equally expressed as in the case of *T. brucei* (*5*).

Heterodimeric forms of T. brucei 14-3-3 proteins are the most stable structures in vivo

We applied BN-PAGE analyses to PCF-cell clones expressing non-tagged 14-3-3I and/or II proteins under the control of tetracycline (Tet) in combination with western blotting using isoform-specific serum. Endogenous 14-3-3 proteins, without Tet induction, formed tightly structured dimers that appeared as a discrete 60 kDa band in all three clones (Fig. 1D, lanes 1, 3, 5, 7, 9 and 11 in BN-PAGE). These results clearly indicate that *T. brucei* 14-3-3 proteins exist as dimers *in vivo* under physiological conditions. Induction of 14-3-3I resulted in 7-fold upregulation over the control level (Fig. 1D, lanes 1 and 2 in SDS–PAGE) and produced a 60-kDa band along with a protein smear of 45–120 kDa (Fig. 1D, lane 2 in BN-PAGE). Within this smear, more intense bands corresponding to ~50 kDa, the most likely complexes of 14-3-3I and detergent-bound form of G-250, and ~100 kDa that are possibly dimers of the ~50 kDa bands, were discerned. The abundance and conformation of 14-3-3II in these 14-3-3I overexpressing cells appeared unaffected; this isoform remained as a discrete band of 60 kDa (Fig. 1D, lanes 7 and 8 in SDS–PAGE, and lanes 1 and 2 in BN-PAGE). Induction of 14-3-3II resulted in 10-fold upregulation (Fig. 1D, lanes 9 and 10 in SDS–PAGE) and produced a 60-kDa band with a significant protein smear of 45–500 kDa (Fig. 1D, lane 10 in BN-PAGE). The abundance and conformation of 14-3-3I in these 14-3-3II overexpressing cells remained unaffected (Fig. 1D, lanes 3 and 4 in both SDS–PAGE and BN-PAGE). Simultaneous induction of 14-3-3I and II in the same cells resulted in a ~7-fold upregulation of both proteins above the control level (Fig. 1D, lanes 5, 6, 11 and 12 in SDS–PAGE). It also gave rise to an intensified 60 kDa band for 14-3-3I and II heterodimers along with smears of 45–120 and 50–180 kDa for monomeric or loosely homodimerized 14-3-3I and II, respectively (Fig. 1D, lanes 6 and 12 in BN-PAGE). Within this smear, more intense bands corresponding to sizes of ~100 kDa were discerned. Although specific antibodies to 14-3-3I and II detected the similar heterodimerized bands with the smear in BN-PAGE followed by western blotting (Fig. 1D, lanes 6 and 12 in BN-PAGE), they are not completely identical, as induction levels of II might be higher than those of I. In comparison with the co-expression of 14-3-3I and II, the expression of 14-3-3I alone showed more diffuse intense bands of ~50 kDa (Fig. 1D, lane 2 in BN-PAGE). The diffuse intense bands are likely composed of the complexes of G-250 and detergent with 14-3-3 monomers as demonstrated in the recombinant 14-3-3ζ S58D proteins that exist as monomeric forms (Fig. 1A). BN-PAGE analyses of *T. brucei* 14-3-3-expressing HEK293T cells resulted in consistent data (Supplementary Fig. S3), also supporting that *T. brucei* 14-3-3 proteins tend to stably heterodimerize when both isoforms are equally expressed as in the case of *T. brucei* (*5*). As both proteins are mutually dependent for maintaining their steady state levels in BSF cells (*5*) and PCF cells, our results further confirm that *T. brucei* 14-3-3 isoforms have a mutual chaperone-like activity.

The 14-3-3 protein–ligand complex contains both I and II isoforms

We have shown difopein, a universal peptide–ligand for 14-3-3, only binds to 14-3-3I but not to 14-3-3II by GST pulldown assay (Supplementary Fig. S4A). Then, we established Tet-inducible EYFP (A5) and EYFP-difopein (E5)-expressing cell clones (Supplementary Fig. S4B). The immunoblot data indicated that anti-EGFP antibodies specifically immunoprecipitated

EYFP-difopein together with the heterodimer complex of 14-3-3I (lower band) and II (higher band) (Fig. 2A, left panel). We also confirmed the contents of immunoprecipitated 14-3-3 proteins using a specific anti-serum to each isoform (Fig. 2B). The efficiency of immunoprecipitation was evaluated by the detection of EYFP and EYFP-difopein in the immunoprecipitates (Fig. 2A, right panel). These data indicate that a significant proportion of *T. brucei* 14-3-3 proteins exists as heterodimers *in vivo*, because 14-3-3II was also recovered effectively in spite of the lack of direct interaction with difopein. In addition, we have previously shown p31-SAP complexes also contain both 14-3-3I and II (*20*). Combined with the data of BN-PAGE analyses, we conclude that majority of *T. brucei* 14-3-3 proteins exist as heterodimeric forms *in vivo*.

Expression of the heterodimer but not the homodimers of T. brucei 14-3-3 is critical for cytokinesis

We have described the phenotype of cells in which 14-3-3 genes expression is depleted, namely, abnormalities in motility, cytokinesis and the cell cycle (*5*). Then, we examined the effects of overexpression of each isoform. In the Tet-inducible clone 14-3-3I F2, the levels of 14-3-3I increased by 12-fold, whereas the levels of 14-3-3II remained constant (1.3-fold) upon Tet induction (Fig. 3A). In the Tet-inducible clone 14-3-3II B11, the levels of 14-3-3II increased by 5.9-fold, whereas the levels of 14-3-3I remained constant (1.2-fold) upon Tet induction (Fig. 3A). Overexpression of each isoform had minimum effects on cell growth and morphologies; the majority of cells showed the 1N/1K (N and K represent nucleus and kinetoplast, respectively) phenotype in both Tet (−) and Tet (+) conditions, while fewer than 10% of cells showed abnormal numbers of N/K, including 0N/1K, 0N/2K, 1N/0K, 2N/0K, 2N/1K and >2N/>2K (Fig. 3B, left and middle panels). We tested two other clones and obtained similar growth curves and morphologies (data not shown). Then, we examined whether overexpression of both isoforms affect cell growth and morphologies. The expression levels of both isoforms in the clone A11 increased 7.5-fold for 14-3-3I and 5.0-fold for 14-3-3II upon Tet induction (Fig. 3A, clone A11) where increased levels were less than that of each isoform expressed alone (Fig. 3A, clones F2 and B11). Surprisingly, there was a clear impact on cell growth and morphology when both isoforms were expressed. The reduction in cell number was almost 10-fold on Day 3 after Tet induction in A11 clone, and abnormal N/K numbers, including 0N/1K, 0N/2K, 1N/0K, 2N/0K, 2N/1K and >2N/>2K, were seen in ~75% of cells on Day 1. A typical abnormal cell is shown in the fluorescence images of clone A11 (Fig. 3B, right panel, Tet+ and Fig. 3C), suggesting that cell division, but not nuclear division, was greatly hampered in these cells. We analysed two additional clones and obtained similar results (Supplementary Fig. S5A and B). As the expressed 14-3-3I and II were less than that expressed in the F2 or B12 clone where single isoform was expressed upon Tet induction, it is less likely that expressed isoforms in the A11 clone individually affected cell growth and morphologies. Rather, these data demonstrate that the heterodimerization of 14-3-3 helps not only to maintain the steady-state levels of the isoforms but also to efficiently control the cell cycle and cytokinesis. Combined with our previous report, these results indicate that a tightly regulated level of 14-3-3 heterodimers in *T. brucei* is important for normal cell cycle progression.

Discussion

Homo- or heterodimerization is among the most important features for the function of 14-3-3 proteins (*9–12*). However, no reports concerning the dimerization of protozoan 14-3-3 proteins, including *T. brucei* 14-3-3, have been published. We first showed that

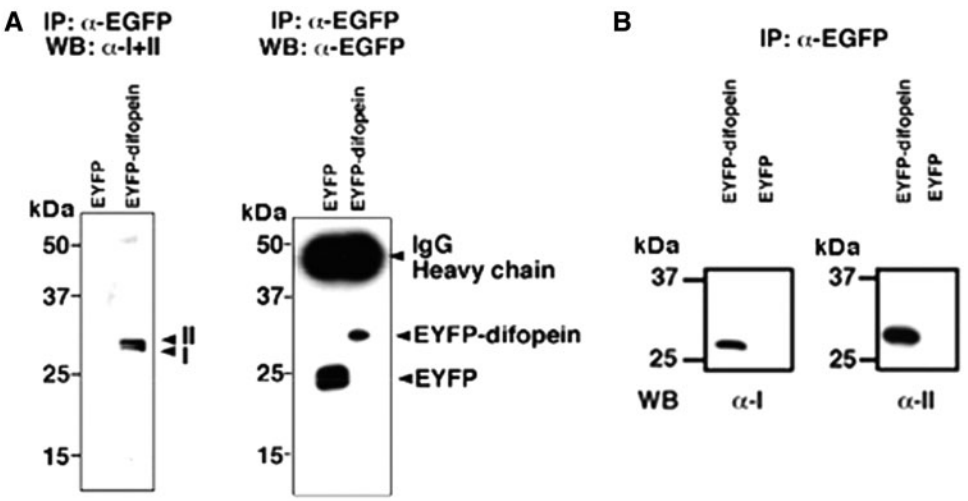

Fig. 2 ***In vivo*** **association of difopein with 14-3-3I and II heterodimer**. (**A**) Immunoprecipitation with anti-EGFP antibodies was carried out using lysates of *T. brucei* clones. Clone A5 expresses EYFP, and clone E5 expresses EYFP-difopein. Blots were probed with a mixture of α-I and II sera (left) and α-EGFP antibodies (right). (**B**) Proteins immunoprecipitated with α-EYFP antibodies were detected with α-I (left) and α-II (right)-specific sera.

T. brucei 14-3-3 proteins form hetero- and homodimers by overexpressing epitope-tagged 14-3-3 proteins. However, two problems may complicate the analysis of the physiological state of hetero- and/or homodimerization of 14-3-3 proteins using this approach. One caveat is that N-terminal and/or C-terminal epitope tags may interfere with or facilitate dimerization. For example, we found that an N-terminal Myc-tag on 14-3-3II interfered with both hetero- and homodimerization, whereas a C-terminal Myc-tag on 14-3-3II facilitates homodimerization. Another example is that a deletion mutant lacking the unique

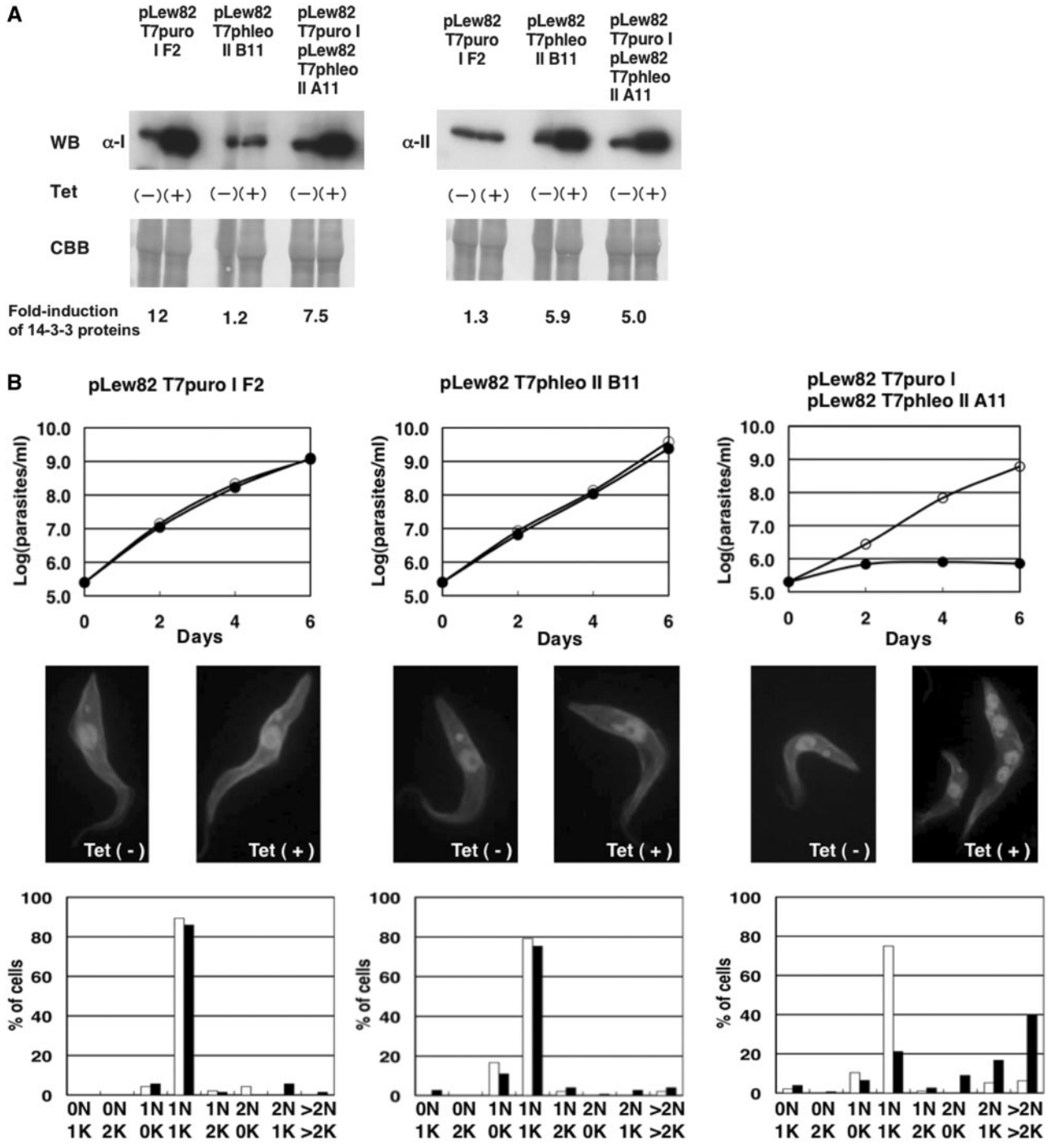

Fig. 3 (**A**) Quantification of the levels of 14-3-3 proteins in *T. brucei* PCF cell clones on Day 1 after Tet induction. Lysates of Tet-induced and/or uninduced clone were made and subjected to western blotting using the indicated antibodies. Quantification was performed using Fluorchem (AlphaInnotech). Fold inductions are shown at the bottom. (**B**) Growth curves of Tet-induced (closed circle) and/or uninduced cell clones (open circle) (upper panel). Typical morphologies of each clone: on Day 1 following Tet induction, cells were fixed and stained with anti-α-tubulin (FITC) and DAPI (middle panel). The numbers of nuclei and kinetoplasts stained with DAPI were counted in 100 cells using fluorescence images (middle panel). The *x*-axis and *y*-axis represent the number of nuclei (N) and kinetoplasts (K), and the fraction of the cells as percentage, respectively. The open and closed bars represent the numbers of Tet-uninduced and Tet-induced cells, respectively (lower panel).

(continued)

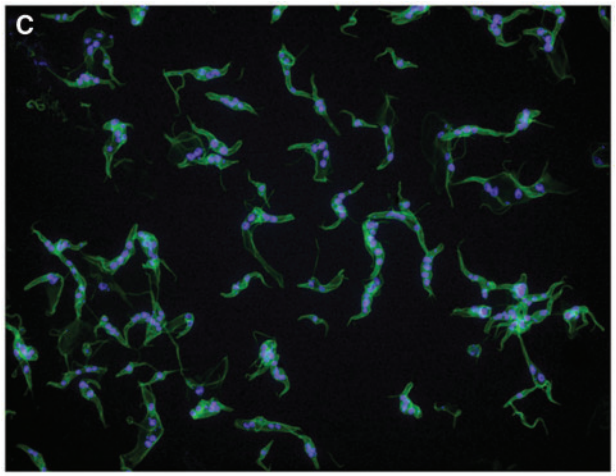

Fig. 3 (**C**) Large fields of the fluorescence images of the clone A11 shown in (**B**).

N-terminal 20 amino acid residues of 14-3-3I cannot form dimers when N-terminal 6xMyc-tag or C-terminal Myc + S-tag fusion is used, but it can form dimers when a C-terminal 2xMyc tag is used (data not shown). Furthermore, overexpression of one isoform leaves excess protein without a potential binding partner(s), possibly resulting in artifacts.

We found that the BN-PAGE system is a useful tool for assessing the dimerization state of non-tagged 14-3-3 proteins under physiological conditions; monomer or loosely structured dimeric 14-3-3 proteins may appear as protein smears, while tightly structured dimeric 14-3-3 proteins may appear as a single discrete band. The BN-PAGE analyses of overexpressed 14-3-3 proteins showed that the heterodimeric form of 14-3-3I and II isoforms is the most stable complex, followed by the 14-3-3I homodimer. We found little evidence for formation of a stable 14-3-3II homodimer.

We also showed that the heterodimeric form of *T. brucei* 14-3-3 has the most potent effect on the cell cycle. Besides periodic nuclear events (G1, S, G2 and M phases), trypanosomes exhibit a periodic S phase for the kinetoplast, and segregation of the kinetoplast before mitosis is a useful marker of cell cycle progression. In addition, *T. brucei* cytokinesis is independent of both mitosis and nuclear DNA synthesis (*21*). Therefore, defects in many biochemical events, including knockdown of phosphatidylinositol 4-kinase (*22*), cathepsin B (*23*) or serine palmitoyltransferase (SPT2) (*24*) gene expression, and chemicals such as okadaic acid (*25*) or vinca alkaloids (*26*) that disrupt the microtubular network, may lead to the production of cells with multiple kinetoplasts and multiple nuclei (>2N >2K). Although we have been able to obtain several binding partners of *T. brucei* 14-3-3 proteins (*20*), we could not explain why the overexpression and the knockdown of the 14-3-3 genes give rise to similar multinucleated cells. However, lack or excess of tightly regulated signal(s) could give rise to a similar phenotype. Although the heterodimer seems to be the functional structure of *T. brucei* 14-3-3 proteins, we cannot exclude the possibility that homodimers have an additional function, because there is evidence that the knockdown of each isoform produces different phenotypes (*5*). Heterodimeric 14-3-3 proteins play more pivotal roles than monomeric or homodimeric forms in *T. brucei* and it could hold true for other kinetoplastid pathogens such as *Trypanosoma cruzi* and *Leishmania major* because of the similarities of 14-3-3 sequences.

Supplementary Data

Supplementary Data are available at *JB* Online.

Acknowledgements

We thank Dr George Cross for pLew82 vector and 29-13 cells, and Dr Haian Fu for pEYFP-difopein (pscm138) vector.

Funding

This work was supported by Ministry of Education, Culture, Sports, Science and Technology grant 23590500 and a collaboration grant of the Institute for Enzyme research, Tokushima (24-12) to M.I.

Conflict of interest

None declared.

References

1. Pozuelo Rubio, M., Geraghty, K.M., Wong, B.H., Wood, N.T., Campbell, D.G., Morrice, N., and Mackintosh, C. (2004) 14-3-3-affinity purification of over 200 human phosphoproteins reveals new links to regulation of cellular metabolism, proliferation and trafficking. *Biochem. J.* **379**, 395–408
2. van Hemert, M.J., Steensma, H.Y., and van Heusden, G.P. (2001) 14-3-3 proteins: key regulators of cell division, signalling and apoptosis. *Bioessays* **23**, 936–946
3. Yaffe, M.B. (2002) How do 14-3-3 proteins work?—Gatekeeper phosphorylation and the molecular anvil hypothesis. *FEBS Lett.* **513**, 53–57
4. Tzivion, G. and Avruch, J. (2002) 14-3-3 proteins: active cofactors in cellular regulation by serine/threonine phosphorylation. *J. Biol. Chem.* **277**, 3061–3064
5. Inoue, M., Nakamura, Y., Yasuda, K., Yasaka, N., Hara, T., Schnaufer, A., Stuart, K., and Fukuma, T. (2005) The 14-3-3 proteins of *Trypanosoma brucei* function in motility, cytokinesis, and cell cycle. *J. Biol. Chem.* **280**, 14085–14096
6. Rosenquist, M., Alsterfjord, M., Larsson, C., and Sommarin, M. (2001) Data mining the *Arabidopsis* genome reveals fifteen 14-3-3 genes. Expression is demonstrated for two out of five novel genes. *Plant Physiol.* **127**, 142–149
7. Aitken, A. (2006) 14-3-3 proteins: a historic overview. *Semin. Cancer Biol.* **16**, 162–172
8. Chaudhri, M., Scarabel, M., and Aitken, A. (2003) Mammalian and yeast 14-3-3 isoforms form distinct patterns of dimers in vivo. *Biochem. Biophys. Res. Commun.* **300**, 679–685
9. Powell, D.W., Rane, M.J., Joughin, B.A., Kalmukova, R., Hong, J.H., Tidor, B., Dean, W.L., Pierce, W.M., Klein, J.B., Yaffe, M.B., and McLeish, K.R. (2003) Proteomic identification of 14-3-3zeta as a mitogen-activated protein kinase-activated protein kinase 2 substrate: role in dimer formation and ligand binding. *Mol. Cell Biol.* **23**, 5376–5387

10. Powell, D.W., Rane, M.J., Chen, Q., Singh, S., and McLeish, K.R. (2002) Identification of 14-3-3zeta as a protein kinase B/Akt substrate. *J. Biol. Chem.* **277**, 21639–21642
11. Megidish, T., Cooper, J., Zhang, L., Fu, H., and Hakomori, S. (1998) A novel sphingosine-dependent protein kinase (SDK1) specifically phosphorylates certain isoforms of 14-3-3 protein. *J. Biol. Chem.* **273**, 21834–21845
12. Woodcock, J.M., Murphy, J., Stomski, F.C., Berndt, M.C., and Lopez, A.F. (2003) The dimeric versus monomeric status of 14-3-3zeta is controlled by phosphorylation of Ser58 at the dimer interface. *J. Biol. Chem.* **278**, 36323–36327
13. Shen, Y.H., Godlewski, J., Bronisz, A., Zhu, J., Comb, M.J., Avruch, J., and Tzivion, G. (2003) Significance of 14-3-3 self-dimerization for phosphorylation-dependent target binding. *Mol. Biol. Cell* **14**, 4721–4733
14. Liu, D., Bienkowska, J., Petosa, C., Collier, R.J., Fu, H., and Liddington, R. (1995) Crystal structure of the zeta isoform of the 14-3-3 protein. *Nature* **376**, 191–194
15. Wirtz, E., Leal, S., Ochatt, C., and Cross, G.A. (1999) A tightly regulated inducible expression system for conditional gene knock-outs and dominant-negative genetics in *Trypanosoma brucei*. *Mol. Biochem. Parasitol.* **99**, 89–101
16. Schagger, H. and von Jagow, G. (1991) Blue native electrophoresis for isolation of membrane protein complexes in enzymatically active form. *Anal. Biochem.* **199**, 223–231
17. Zhang, L., Wang, H., Liu, D., Liddington, R., and Fu, H. (1997) Raf-1 kinase and exoenzyme S interact with 14-3-3zeta through a common site involving lysine 49. *J. Biol. Chem.* **272**, 13717–13724
18. Gu, Y.M., Jin, Y.H., Choi, J.K., Baek, K.H., Yeo, C.Y., and Lee, K.Y. (2006) Protein kinase A phosphorylates and regulates dimerization of 14-3-3 epsilon. *FEBS Lett.* **580**, 305–310
19. Meller, N., Liu, Y.C., Collins, T.L., Bonnefoy-Berard, N., Baier, G., Isakov, N., and Altman, A. (1996) Direct interaction between protein kinase C theta (PKC theta) and 14-3-3 tau in T cells: 14-3-3 overexpression results in inhibition of PKC theta translocation and function. *Mol. Cell Biol.* **16**, 5782–5791
20. Inoue, M., Yasuda, K., Uemura, H., Yasaka, N., Inoue, H., Sei, Y., Horikoshi, N., and Fukuma, T. (2010) Phosphorylation-dependent protein interaction with *Trypanosoma brucei* 14-3-3 proteins that display atypical target recognition. *PLoS One* **5**, e15566
21. Ploubidou, A., Robinson, D.R., Docherty, R.C., Ogbadoyi, E.O., and Gull, K. (1999) Evidence for novel cell cycle checkpoints in trypanosomes: kinetoplast segregation and cytokinesis in the absence of mitosis. *J. Cell. Sci.* **112 (Pt 24)**, 4641–4650
22. Rodgers, M.J., Albanesi, J.P., and Phillips, M.A. (2007) Phosphatidylinositol 4-kinase III-beta is required for Golgi maintenance and cytokinesis in *Trypanosoma brucei*. *Eukaryot. Cell* **6**, 1108–1118
23. Mackey, Z.B., O'Brien, T.C., Greenbaum, D.C., Blank, R.B., and McKerrow, J.H. (2004) A cathepsin B-like protease is required for host protein degradation in *Trypanosoma brucei*. *J. Biol. Chem.* **279**, 48426–48433
24. Fridberg, A., Olson, C.L., Nakayasu, E.S., Tyler, K.M., Almeida, I.C., and Engman, D.M. (2008) Sphingolipid synthesis is necessary for kinetoplast segregation and cytokinesis in *Trypanosoma brucei*. *J. Cell. Sci.* **121**, 522–535
25. Das, A., Gale, M. Jr., Carter, V., and Parsons, M. (1994) The protein phosphatase inhibitor okadaic acid induces defects in cytokinesis and organellar genome segregation in *Trypanosoma brucei*. *J. Cell. Sci.* **107 (Pt 12)**, 3477–3483
26. Grellier, P., Sinou, V., Garreau-de Loubresse, N., Bylen, E., Boulard, Y., and Schrevel, J. (1999) Selective and reversible effects of vinca alkaloids on *Trypanosoma cruzi* epimastigote forms: blockage of cytokinesis without inhibition of the organelle duplication. *Cell Motil. Cytoskeleton* **42**, 36–47